

Experimental evaluation of mechanical properties and machine process in Fused Deposition Modelling printed polymeric elements

Original

Experimental evaluation of mechanical properties and machine process in Fused Deposition Modelling printed polymeric elements / Brischetto, Salvatore; Torre, Roberto; Ferro, CARLO GIOVANNI. - 975:(2019), pp. 377-389. (Intervento presentato al convegno AHFE 2019 International Conference on Additive Manufacturing, Modeling Systems and 3D Prototyping tenutosi a Washington D.C. (USA) nel July 24–28 2019) [10.1007/978-3-030-20216-3_35].

Availability:

This version is available at: 11583/2745093 since: 2020-06-15T09:59:04Z

Publisher:

Springer Nature Switzerland AG 2020

Published

DOI:10.1007/978-3-030-20216-3_35

Terms of use:

This article is made available under terms and conditions as specified in the corresponding bibliographic description in the repository

Publisher copyright

(Article begins on next page)

Experimental Evaluation of Mechanical Properties and Machine Process in Fused Deposition Modelling Printed Polymeric Elements

Salvatore Brischetto¹, Roberto Torre¹ and Carlo Giovanni Ferro¹

¹ Department of Mechanical and Aerospace Engineering, Politecnico di Torino,
Corso Duca degli Abruzzi 24, 10129 Torino, Italy
{salvatore.brischetto, roberto.torre, carlo.ferro}@polito.it

Abstract. In this paper, the consolidation of an experimental approach for the evaluation of the mechanical properties of FDM (Fused Deposition Modelling) 3D printed objects is proposed. ASTM standards addressed to polymers were adapted to FDM 3D printed specimens in order to derive a complete mechanical characterization of PLA (PolyLactic Acid). The tensile test aimed to the determination of the in-plane mechanical properties of pseudo-isotropic specimens. The compression test allowed the evaluation of the out-of-plane mechanical properties of 3D printed parts. The three-point bending test on sandwich specimens helped to assess the not studied potential of FDM in the production of complex and integrated structural elements. The quantitative results show that this common, non-structural, environmentally friendly polymer can be successfully employed to produce customized and integrated structural elements for non-critical operating environment.

Keywords: Fused Deposition Modelling (FDM) · 3D printing process · Additive Manufacturing · Mechanical Properties · Tensile Test · Compression Test · Bending Test · PolyLactic Acid (PLA) · Sandwich Structures · Honeycomb Core

1 Introduction

The Fused Deposition Modelling (FDM) technology belongs to the family of Additive Manufacturing processes for polymeric materials. It is widely used for rapid prototyping. Recent years saw a growing interest in this technology, accompanied by the attempt to use it also for functional and structural parts. One of the limits of this technology is that it has a strong influence on the mechanical properties of the finished pieces. The knowledge of the mechanical properties of the bulk material is not sufficient and the actual properties of the printed parts need to be experimentally determined as a function of the printing parameters. In previous works, the present authors proposed a tensile [1] and compression [2] characterization of ABS. Furthermore, a preliminary analysis of homogeneous and inhomogeneous 3D printed sandwiches was carried out in [3]. This paper aims at a complete characterization of PLA under specific printing conditions. The tensile properties are determined under in-plane load con-

ditions; the compression properties are determined under out-of-plane load conditions. The experimental approach for sandwich specimens proposed in [3] is here consolidated by means of new results.

2 Specimens Production and Printing Parameters

All the specimens were produced using home-desktop 3D printers. The tensile and flexural specimens were printed by means of a Creatbot DX 3D printer. The specimens for compression tests were produced using a Sharebot NG 3D printer. The printing volume of the first 3D printer is 300x250x300mm; the printing volume of the second one is 230x200x200mm. Both the machines are equipped with two extruders. Even if the geometries of the specimens are simple, the present authors noted in previous works [1]-[3] that the process variability in home-desktop 3D printers is pronounced for both the geometrical and mechanical features. The influence of various printing parameters on the mechanical properties of the finished parts is a well-known issue in the literature [4]-[7]. At the same time, the mechanical properties can be affected by non-conformities in the geometry and in the manufacturing process. The values to be associated with the selectable parameters were carefully chosen. A series of calibration tests was done to assess the match between the expected and the real values.

Layer height, H_L : the vertical dimension of the deposited raster can be freely chosen in a certain range; the lower bound is represented by the Z-resolution of the 3D printer, while the upper bound generally coincides with the transverse dimension of the nozzle. Several authors noted that when the layer height is smaller, with respect to the nozzle size, the inter-layer adhesion improves. Consequently, the lowest value was imposed.

Raster width, W_R : as first approximation, the transverse dimension of the deposited raster is only a function of the nozzle diameter and of the layer height. Once the layer height is chosen, the slicing software estimates the raster width under optimum conditions. The actual value under real operating conditions was carefully checked with a thin wall test. The difference between the two values was offset by changing the extrusion multiplier.

Raster angle, R_A : the deposition orientation with respect to the load application direction strongly affects the mechanical performances of 3D printed pieces. Several stacking sequences should be tested in order to build a model that could approximate the phenomenon. In order to evaluate the in-plane mechanical properties, a quasi-isotropic lamination scheme was preliminary chosen in the present work.

Perimeters: the number of peripheral beads was chosen in order to have a negligible impact on the mechanical properties. The peripheral beads follow the contour of the piece. Therefore, they are not homogeneous with the internal infill. The number of perimeters was incremented for the flexural specimens because other geometry-related factors must be considered.

Temperatures, T_{EXT} and T_{BED} : both the extrusion (T_{EXT}) and the bed (T_{BED}) temperatures were set accordingly with the values provided by the manufacturer of the raw material.

Table 1 lists the values associated with each of the presented printing parameter.

Table 1. Printing parameter values for tensile, compression and flexural specimens.

| Spcm TYPE | H _L | W _R | Perimeters | R _A | T _{BED} | T _{EXT} |
|-------------|----------------|----------------|------------|----------------|------------------|------------------|
| Tensile | 0.1 mm | 0.5 mm | 1 | [+45°/-45°] | 200°C | 50°C |
| Compressive | 0.1 mm | 0.5 mm | 1 | [+45°/-45°] | 200°C | 50°C |
| Flexural | 0.1mm | 0.5mm | 3 | [+45°/-45°] | 200°C | 50°C |

3 Tensile test set-up

The aim of this section is the determination of the in-plane tensile properties of PLA components produced using a home-desktop 3D printer under fixed environmental parameters. The guidelines of the Standard Test Method for Tensile Properties of Plastics (ASTM D638 [8]) were strictly followed in the test set-up and in the data post-processing. The standard proposes a set of five different specimens. All the specimens present a similar dog-bone geometry; the dimensions change as a function of the thickness. The standard points out that the thickness of the available material should be used to determine the appropriate specimen geometry. This requirement is not relevant for FDM 3D printed parts because the desired thickness can be easily selected. Consequently, TYPE I specimen was chosen for the experimental proposed campaign. The drawing of the specimen is given in Figure 1.

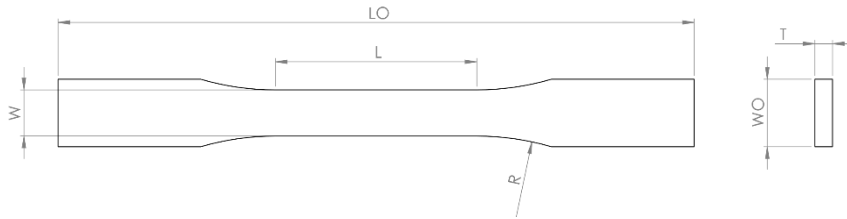


Fig. 1. Sketch of Type I ASTM D638 specimen for tensile test.

The overall length was increased with respect to the recommended minimum value in order to guarantee a length of at least 40 mm for each side of the grip. The grips of the testing machine are 50 mm long; a gripping area shorter than 40 mm could not allow a proper test. A comparison between the recommended and the actual dimensions of the specimens is proposed in Table 2.

Table 2. Tensile test: comparison between the recommended and the actual specimens dimensions.

| Dimensions | Recommended ASTM D638 TYPE I | Actual (nominal dimensions) |
|-------------------------------------|---------------------------------|--------------------------------|
| W – width of narrow section | 13 mm | 13 mm |
| L – length of narrow section | 57 mm | 57 mm |
| W _O – overall width, min | 19 mm | 19 mm |

| | | |
|--------------------------|--------|--------|
| LO – overall length, min | 165 mm | 180 mm |
| R – radius of fillet | 76 mm | 76 mm |
| T - thickness | - | 5 mm |

The number of tested specimens was increased from the requested minimum value of 5 to 10 in order to obtain more statistically stable results.

As anticipated in Section 2, all the specimens present the same $[+45^{\circ}/-45^{\circ}]$ stacking sequence. The use of one single peripheral bead is necessary to have a better surface finish, in order to avoid premature failures due to stress concentrations between adjacent beads at the specimen edges. For the entire length of the narrow section, the perimeters are oriented along the specimen longitudinal axis, this axis coincides with the load application direction during the tensile test. Two beads (one for each side) are 1 mm wide. Therefore, it can be assumed that they play a negligible influence over the overall width of the narrow section.

3.1 Test set-up

The thickness and the width of the narrow section of each specimen were measured as requested by the ASTM standard. The actual dimensions are compared with the nominal ones in Table 3.

Table 3. Actual tensile specimens dimensions. All the values are in mm.

| n° | 1 | 2 | 3 | 4 | 5 | 6 | 7 | 8 | 9 | 10 | NOM |
|----|-------|-------|-------|-------|-------|-------|-------|-------|-------|-------|-------|
| W | 13.03 | 13.11 | 13.07 | 13.09 | 13.13 | 13.12 | 13.13 | 13.09 | 13.09 | 13.12 | 13.00 |
| T | 5.03 | 4.95 | 4.98 | 4.96 | 4.80 | 4.88 | 4.80 | 4.81 | 4.79 | 4.89 | 5.00 |

The width (W) of the sample was slightly higher than the nominal value; a mean value of 13.10 mm was found with a standard deviation of 0.0312 mm. At the same time, the specimens were slightly thinner than planned; the thickness (T) mean value was 4.89 mm with a higher standard deviation of 0.0875 mm.

Each specimen was placed vertically in the grips of the testing machine. It was checked that the specimen principal axis was aligned with the load application direction. The machine was controlled in speed; the lowest speed of testing for TYPE I specimens was chosen for the lower jaw (4 mm/min). This testing speed caused the specimen fail approximately 1 minute after the beginning of the test.

4 Compression test set-up

The Standard Test Method for Compressive Properties of Rigid Plastics (ASTM D695 [9]) was carefully followed in all its guidelines. A prism or a right cylinder is the prescribed shape to be used to study the compression properties of rigid plastics. While the dimensions of the cross section are prescribed, the length can be chosen as a function of the desired properties. When the compression strength is investigated, the length should be twice the specimen principal width or diameter. In the case of the

compression elastic modulus, the standard proposes longer specimens with slenderness ratio between 11:1 and 16:1¹.

In the framework of the present paper, a prism specimen was chosen in order to have a comparable study with previous authors' work for [2]. The slenderness ratio was limited to the lowest value to reduce or delay the occurrence of the buckling phenomenon. Figure 2 presents the drawing of the specimen, and the relevant quotes.

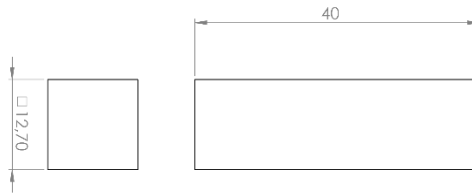


Fig. 2. Sketch of ASTM D695 specimen for modulus measurements for compression test.

The specimens were printed with the square cross section resting upon the printing bed. This feature allows the determination of the out-of-plane compressive properties of PLA. The used lamination scheme is the same of the previous specimens. Layers with raster angle of $+45^\circ$ and -45° were combined. A single perimeter was used to improve the surface finish and to avoid its negative effects.

4.1 Test set-up

The cross section and the height of each specimen were measured before the test. Table 4 shows the smallest section values of each specimen and the global length.

Table 4. Actual compression specimens dimensions. All the values are in mm.

| n° | 1 | 2 | 3 | 4 | 5 | 6 | 7 | 8 | 9 | 10 | NOM |
|-------|-------|-------|-------|-------|-------|-------|-------|-------|-------|-------|-------|
| W_x | 12.84 | 12.85 | 12.84 | 12.68 | 12.79 | 1.76 | 12.83 | 12.88 | 12.85 | 12.67 | 12.70 |
| W_y | 12.65 | 12.8 | 12.66 | 12.61 | 12.66 | 12.63 | 12.72 | 12.69 | 12.84 | 12.64 | 12.70 |
| H | 39.98 | 39.86 | 39.84 | 39.79 | 39.91 | 39.83 | 39.87 | 39.81 | 39.77 | 39.80 | 40.00 |

The nominal dimension of the square cross-section was 12.70 mm. Along the X-printer direction (W_x), the sample showed a mean value of 12.80 mm. The dimensions collected along the Y-printer direction (W_y) give a mean value of 12.69 mm. The standard deviation was almost the same for the two in-plane dimensions: 0.0734 mm was registered along the first mentioned direction and 0.0756 mm along the second one. All the specimens were shorter than the expected value; a mean height of 39.85 mm was registered with a standard deviation of 0.0628 mm.

¹ The slenderness ratio of a solid with constant cross-section can be calculated dividing its length by its minimum radius of gyration.

The specimens were placed individually between the two plane supports of the testing machine. The standard speed for this type of test (1.3 mm/min proposed by the ASTM standard) was used. All the specimens reached the peak stress between the second and the third minute of testing.

5 The flexural test

A three-point bending test was executed strictly following the Standard Test Methods for Flexural Properties of Unreinforced and Reinforced Plastics (ASTM D790 [10]). This method allows to determine both the flexural modulus and the flexural strength; these properties can be determined only for those specimens that fail or break in the outer surface within the 5% strain limit. For thickness values equal or greater than 1.6 mm, the specimen takes the form of a beam with constant rectangular cross-section. Specimen dimensions must be determined as a function of the span between the two testing supports used for the test. Support span and specimen depth shall have a ratio of 16:1. For specimens with thickness greater than 3.2 mm, the width should be less than $\frac{1}{4}$ of the support span. The overall length of the specimen should consider an enough overhang with respect to the supports on both sides. Table 5 gives the recommended and actual specimen dimensions.

Table 5. Flexural test: comparison between the recommended and the actual specimens dimensions.

| Dimensions | Recommended ASTM D790 | Actual (nominal dimensions) |
|---------------------|--------------------------|--------------------------------|
| L – support span | - | 90 mm |
| LO – overall length | - | 105 mm |
| W – width | $< L/4$ | 22.52 mm |
| D – depth | $L/16$ | 5 mm |

In a previous research [3], the present authors assessed the feasibility of sandwich structures produced with a home desktop 3D printer. Several sandwich configurations were tested. A homogeneous sandwich, embedding PLA for the skins and for the honeycomb core, printed with the same extruder; a heterogeneous sandwich, embedding PLA for the honeycomb core and ABS for the skins; a heterogeneous sandwich, embedding PLA for the homogeneous core and ABS for the skins; a homogeneous sandwich, embedding PLA for both the skins and the honeycomb core, where each one was printed with a different extruder. It was supposed that the use of two different extruders, one for the skins and one for the core, could give lower mechanical performances due to a bad adhesion between the layers.

In order to complete a homogeneous mechanical characterization of 3D printed PLA, the homogeneous configuration, with PLA skins and PLA honeycomb core, was here chosen. The honeycomb core is 3 mm thick; the upper and lower skins symmetrically occupy the remaining thickness. A hexagon with an apothem of 2.5 mm represents the repeating geometrical element of the core. The walls of each cell are 0.5mm thick. Figure 3 shows the 2D drawing of the produced specimens. 10 specimens in place of

the minimum requested number of 5, were printed and tested to obtain a bigger sample.

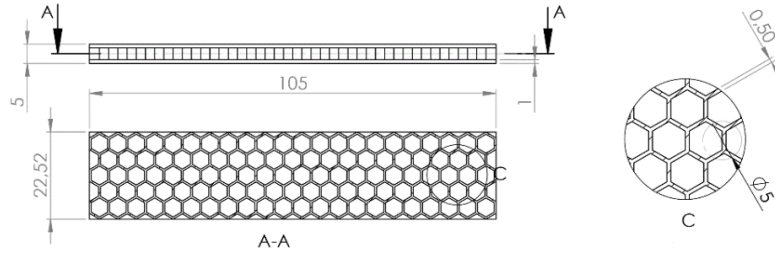


Fig. 3. Sketch of the flexural specimen with sandwich configuration.

As anticipated in Section 2, this specimen configuration has certain peculiarities that must be considered for production. The skins kept the $[+45^\circ/-45^\circ]$ lamination sequence. However, this lamination scheme was not possible for the core because of the reduced dimension of the walls of the hexagonal cells. The upper skin needed an extra attention because it does not lie on a planar and homogeneous surface, but it must be built on mid-air. In order to achieve best printing results, the printer fan was kept on when the first layer was being printed. This feature allows the extruded plastic to harden quickly. Furthermore, the number of perimeters was increased to 3 in order to produce right angles.

5.1 Test set-up

The geometrical dimensions of each specimen were measured with a digital caliper. Both the depth and the width are necessary to calculate the desired mechanical properties. Furthermore, they can be useful to assess the reliability of the manufacturing process for repeating elements. Table 6 collects the measured dimensions.

Table 6. Actual flexural specimen dimensions. All the values are in mm.

| n° | 1 | 2 | 3 | 4 | 5 | 6 | 7 | 8 | 9 | 10 | NOM |
|----|--------|--------|--------|--------|--------|--------|--------|--------|--------|--------|-------|
| LO | 105.01 | 104.88 | 104.89 | 104.85 | 104.82 | 104.97 | 104.94 | 104.81 | 104.85 | 104.89 | 105 |
| W | 23.02 | 23.07 | 23.07 | 23.03 | 23.06 | 23.02 | 23.01 | 23.06 | 23.01 | 23.04 | 22.52 |
| D | 4.85 | 4.81 | 4.84 | 4.82 | 4.88 | 4.81 | 4.88 | 4.80 | 4.85 | 4.81 | 5 |

For the overall length (LO), the nominal value of 105mm and a mean value of 104.89 mm was found with a standard deviation of 0.0649 mm. The nominal width (W) was supposed to be equal to 22.52 mm, a mean value of 23.04 mm with a standard deviation of 0.0242 mm was found. For the depth (D), a nominal value of 5 mm was required, but a mean value of 4.84 mm, with a standard deviation of 0.0295 mm, was obtained.

Each specimen was positioned horizontally, with the lower surface resting on two supports symmetrically positioned with respect to the specimen centerline. A vertical nose acting on the upper surface by loading each specimen right over its centerline. A deflectometer was used to measure the deflection of the specimen under its centerline. By following Procedure A of ASTM D790 standard, the rate of the cross-head motion was calculated imposing a rate of straining of the outer fibers equal to 0.01 mm/mm/min:

$$R = ZL^2/6d . \quad (1)$$

In Eq. (1), d is the actual depth of the specimen, L is the distance between the two supports of the testing machine and Z is the rate of straining of the outer fibers. In order to be applicable, Procedure A requires that the specimen break or yield at a strain lower than 5.0%. This requirement can be translated in terms of deflection of the specimen using:

$$D = rL^2/6d . \quad (2)$$

L and d have the same meaning of Eq. (1); r represents the strain of the outer fibers, which was set equal to 5.0%. For a specimen with the nominal geometrical dimensions, Procedure A requires that the failure occurs for a deflection less than 13.5 mm. As it will be shown in the result section, all the specimens were compliant to this requirement.

6 Results

The present section is devoted to the discussion of the numerical results obtained with the post-processing of the raw data. The Data Acquisition System of the test machine sampled the applied load and the displacement of the lower jaw every tenth of second. For the tensile and the compression test, the load was converted to a uniaxial stress simply dividing it by the cross section dimension of the respective specimen (according to the geometric dimensions reported in Tables 3 and 4). As no strain gauge was used to measure the strains, they were estimated dividing the displacement by the initial length. For tensile specimens, the initial length was assumed to be the length of the narrowed section. For compression specimens, the initial length was considered equal to the lengths reported in Table 4. In the case of the flexural test, the machine reported the applied load and the deflection of the central nose. The load configuration, the boundary conditions and the geometry are obtained considering that the maximum stress and the maximum strain occur in correspondence to the midpoint of the outer surface. The stress was calculated using:

$$\sigma_f = 3PL/2wd^2 . \quad (3)$$

P is the load applied by the testing machine; w is the width of the specimen and d its depth. L is the support span of the testing machine. The strain was obtained via the following relation:

$$\varepsilon_f = 6Dd/L^2 . \quad (4)$$

D is the measured deflection; the other quantities have the same meaning seen in Eq. (3).

For the three tests, the modulus of elasticity was calculated with a linear regression by gradually increasing range of values. At each iteration, the new coefficient was averaged with the previous ones. The procedure was stopped when the new coefficient differs more than 5% from the last calculated mean value. The stress corresponding to this point was identified as the proportional limit stress.

For each of the three tests, an example of the stress-strain curve is proposed. The recorded modulus of elasticity, the strength and the proportional limit (where available) are proposed for each specimen in each test.

6.1 Tensile test

Table 7 summarizes the results collected for the entire sample. The stress-strain curve for tensile specimen n° 3 is shown in Figure 4.

Table 7. Experimental data for tensile specimens.

| n° | 1 | 2 | 3 | 4 | 5 | 6 | 7 | 8 | 9 | 10 | |
|----------------|------|------|------|------|------|------|------|------|------|------|----------------------|
| E | 2918 | 2764 | 2857 | 2722 | 2731 | 2733 | 2749 | 2834 | 2766 | 2704 | [N/mm ²] |
| σ_{max} | 55.3 | 57.8 | 55.7 | 54.5 | 54.6 | 53.4 | 56.0 | 55.2 | 53.8 | 53.5 | [N/mm ²] |
| σ_{pro} | 27.3 | 30.2 | 29.8 | 27.8 | 29.7 | 30.3 | 29.5 | 30.1 | 29.5 | 28.7 | [N/mm ²] |

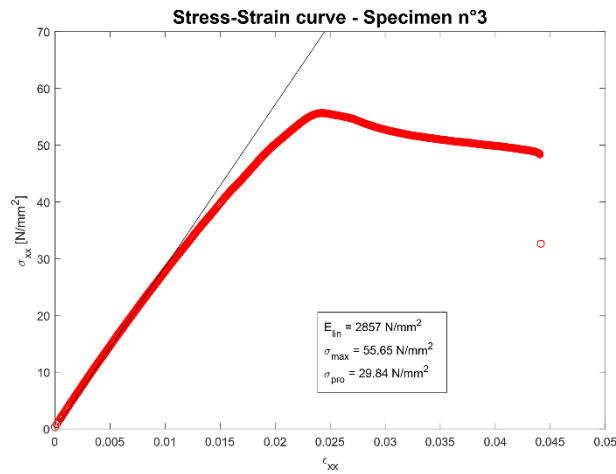


Fig. 4. Post-processed stress-strain curve for the tensile test of specimen 3.

All the ten specimens presented the classical linear-elastic region. At about half the value of the maximum stress, the curve starts to deviate from the linearity, with the tangent modulus decreasing when the stress increases. The maximum stress represents an inflection point. After it, the rest of the curve is concave upward. A small discrete plastic region is present. The tensile modulus E_{in} registered a mean value of 2778

N/mm² with a standard deviation of 69.1 N/mm². A mean value of 55.0 N/mm² was recorded for the maximum strength σ_{\max} , with a standard deviation of 1.3 N/mm². For the tensile limit of elasticity σ_{pro} , a mean value of 29.3 N/mm², with a standard deviation of 1.0 N/mm², was found.

6.2 Compression test

The mechanical characteristics of the sample are presented in Table 8. Figure 5 gives the actual recorded stress-strain curve for specimen n°2. This figure is representative of the sample behavior.

Table 8. Experimental data for compressive specimens.

| n° | 1 | 2 | 3 | 4 | 5 | 6 | 7 | 8 | 9 | 10 | |
|-----------------------|------|------|------|------|------|------|------|------|------|------|----------------------|
| E | 2385 | 2056 | 2081 | 2166 | 2353 | 2269 | 2089 | 2132 | 2129 | 2173 | [N/mm ²] |
| σ_{\max} | 83.9 | 76.0 | 83.4 | 84.2 | 88.2 | 88.0 | 86.3 | 83.5 | 86.0 | 85.0 | [N/mm ²] |
| σ_{pro} | 83.2 | 73.3 | 81.5 | 83.6 | 85.5 | 86.7 | 83.1 | 81.0 | 81.4 | 82.5 | [N/mm ²] |

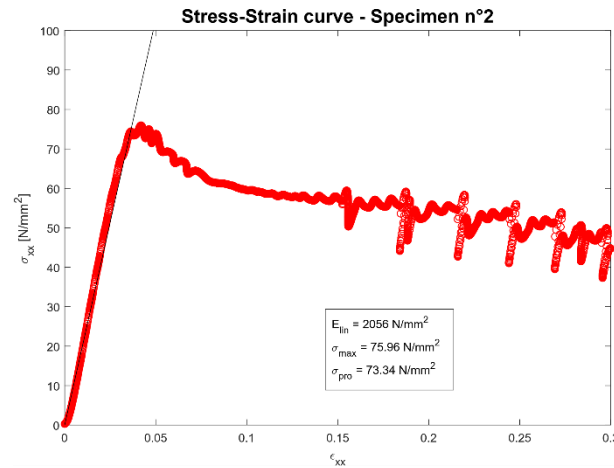


Fig. 5. Post-processed stress-strain curve for the compression test of specimen 2.

The analysis of the raw data shows a mean value for the compressive modulus of elasticity E_{lin} equal to 2183 N/mm², with a standard deviation of 114.6 N/mm². The compression maximum stress σ_{\max} has a mean value of 84.5 N/mm², with a standard deviation of 3.4 N/mm². The mean value of the compression limit of elasticity σ_{pro} is very close to the compression strength: it is 82.2 N/mm² with a standard deviation of 3.6 N/mm².

Specimens showed no macroscopically visible deformation until the maximum compression stress was reached. After it, a bulge appears and the deformation becomes visible. The fluctuations showed in Figure 5 were associated to subsequent readjustments of the specimen in its place.

6.3 Flexural test

Table 9 shows the mechanical characteristics for each specimen. The processed stress-strain curve for specimen n° 5 is given in Figure 6.

Table 9. Experimental data for flexural specimens.

| n° | 1 | 2 | 3 | 4 | 5 | 6 | 7 | 8 | 9 | 10 | |
|----------------|------|------|------|------|------|------|------|------|------|------|----------------------|
| E | 2491 | 2325 | 2383 | 2395 | 2307 | 2366 | 2486 | 2358 | 2441 | 2617 | [N/mm ²] |
| σ_{max} | 61.4 | 62.0 | 61.4 | 63.8 | 61.7 | 61.9 | 57.9 | 62.7 | 63.5 | 64.6 | [N/mm ²] |

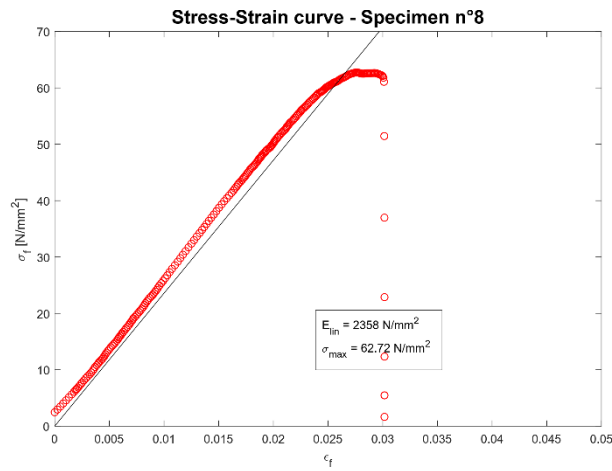


Fig. 6. Post-processed stress-strain curve for the flexural test of specimen 8.

In all the specimens of the sample, the stress-strain curve for the flexural analysis showed a clear linear-elastic region. After the end of the linear region, all the specimens broke. The flexural modulus of elasticity E_{lin} has a mean value of 2417 N/mm² with a standard deviation of 93.7 N/mm². The sample mean value of the flexural strength σ_{max} was 62.1 N/mm², with a standard deviation of 1.8 N/mm².

7 Conclusions and Further Developments

In the proposed work, the consolidation of an experimental approach for the determination of the mechanical properties of 3D printed object was carried out. The in-plane tensile properties of quasi-isotropic FDM 3D printed PLA were determined. Under the specific printing conditions, the in-plane tensile mechanical properties of 3D printed PLA are not so different from their respective values of molded PLA [11]. A mean value of 2778 N/mm² was found for the tensile elastic modulus; the tensile strength reached a mean value of 55 N/mm². The out-of-plane compression elastic modulus was determined, it was 2183 N/mm², that means slightly lower than the in-plane tensile one. A mean value of 84.5 N/mm² was found for the compression maxi-

imum stress. Further studies should be carried out in order to assess if this value is correct (without buckling phenomenon). A study on compression stocky specimens will be proposed in a companion paper to clarify this issue. At the same time, the study of 3D printed PLA compression properties will be extended to in-plane load conditions and, mutually, the study on tensile properties will be extended to out-of-plane load conditions. The flexural properties of sandwich PLA specimens with honeycomb core were studied. The mean values of the flexural modulus of elasticity and of the flexural strength are 2417 N/mm² and 62.1 N/mm², respectively. The flexural stress-strain behavior of the sample was the same recorded in a previous and preliminary study of the same authors [3], even though the mechanical properties of the present sample reached higher values. As explained in Section 5, the manufacture of the upper skin in sandwich 3D-printed specimens is critical as it does not lie on a planar and homogeneous surface. An improved selection of the printing parameters leads to a lower defect concentration in the sample in order to avoid a premature failure.

References

1. Ferro, C.G., Brischetto, S., Torre, R., Maggiore, P.: Characterization of ABS Specimens produced via the 3D Printing Technology for Drone Structural Components. *Curved and Layered Structures*. 3, 172--188 (2016)
2. Brischetto, S., Ferro, C.G., Maggiore, P., Torre, R.: Compression Tests of ABS Specimens for UAV Components Produced via the FDM Technique. *Technologies*. 5, 1--25 (2017)
3. Brischetto, S., Ferro, C.G., Torre, R., Maggiore, P.: 3D FDM Production and Mechanical Behavior of Polymeric Sandwich Specimens embedding Classical and Honeycomb Cores. *Curved and Layered Structures*. 5, 8--94 (2018)
4. Ahn, S.-H., Montero, M., Odell, D., Roundy, S., Wright, P.K.: Anisotropic Material Properties of Fused Deposition Modeling ABS. *Rapid Prototyping Journal*. 8, 248--257 (2002)
5. Raut, S., Kumar, S., Jatti, S., Khedkar N.K., Singh, T.P.: Investigation of the Effect of Built Orientation on Mechanical Properties and Total Cost of FDM Parts, 3rd International Conference on Materials Processing and Characterisation, *Procedia Materials Science*. 6, 1625--1630 (2014)
6. Croccolo, D., De Agostinis, M., Olmi, G.: Experimental Characterization and Analytical Modelling of the Mechanical Behavior of Fused Deposition Processed Parts made of ABS-M30. *Computational Material Science*. 79, 506--518 (2013)
7. Pincini, M.: Caratterizzazione sperimentale di proprietà Meccaniche di component costruiti mediante fused deposition modelling. Bachelor degree thesis in Aerospace Engineering discussed at the Politecnico di Torino. Turin, Italy (2015)
8. ASTM D638-10, Standard Test Method for Tensile Properties of Plastics. Annual Book of ASTM Standards, ASTM International. West Conshohocken, PA, USA (2010)
9. ASTM D695-02, Standard Test Method for Compressive Properties of Rigid Plastics. Annual Book of ASTM Standards, ASTM International. West Conshohocken, PA, USA (2002)
10. ASTM D790-17, Standard Test Method for Flexural Properties of Unreinforced and Reinforced Plastics and Electrical Insulating Materials. Annual Book of ASTM Standards, ASTM International. West Conshohocken, PA, USA (2017)
11. Farah, S., Anderson, D.G., Langer, R.: Physical and Mechanical Properties of PLA, and their Functions in Widespread Applications – A Comprehensive review. *Advanced Drug Delivery Reviews*. 107, 367--392 (2016)